



# Long-term meteorological and hydrological drought characteristics on the lower Tigris-Euphrates basin, Türkiye: relation, impact and trend

Musa Esit<sup>1</sup> · Recep Çelik<sup>2</sup> · Ergun Akbas<sup>2</sup>

Received: 15 December 2022 / Accepted: 6 September 2023 / Published online: 26 September 2023  
© The Author(s), under exclusive licence to Springer-Verlag GmbH Germany, part of Springer Nature 2023

## Abstract

This study aims to provide a comprehensive analysis of meteorological and hydrological droughts in the lower Tigris-Euphrates basin, Türkiye over 12-month time scale using the standardized precipitation index (SPI) and the Standardized Precipitation Evapotranspiration Index (SPEI) and the standardized streamflow index (SDI). To evaluate monthly trends of the SPI, SPEI, and SDI series, Mann–Kendall (MK), Spearman Rho (SR), and innovative trend analysis (ITA) tests are employed. The intrinsic relationships between the hydrological and meteorological drought in the study area as well as the specifics of how the oscillation period changes over time can also be obtained via wavelet transform coherence (WTC), which can reveal essential information. The results of all trend tests performed a decreasing trend consistently at stations 17275, 17810, 17948, 17950, and 17968 for all months in terms of SPI. SPEI is more sensitive to trend detection than SPI when taking into account all trend testing. In addition, the three trend tests are found to be more consistent with each other when SPEI is compared to SPI. According to SDI, the ITA method is clearly superior to the other two methods for identifying hidden trends. The ITA method, for example, captures a considerably increasing/decreasing trend at stations E26A038 (January and February), E26A012 (January, February, and from May to December), and E26A033 (from June to December) despite MK and SR tests finding no significant trends at any of the stations. When considering the WTC, positive month signals are strongly correlated with 12-month periods, according to the majority of stations.

**Keywords** Meteorological drought · Hydrological drought · ITA · Trend · WTC · Lower Tigris-Euphrates basin

## Introduction

Drought is a serious natural disaster (Zhou et al. 2021; Christian et al. 2021; Farrokhi et al. 2021). Climate change has increased the frequency of extreme weather events. In contrast to other natural disasters, drought is a slow-onset danger that affects huge areas over prolonged periods. Drought can have significant effects on ecological stability and social growth (Yuan et al. 2017; Xu et al. 2019; King-Okumu et al. 2020; Zhou et al. 2020). In terms of the evolution of a drought, the key contributing factor is a long-term

precipitation deficit, which may also result further in a lack of soil moisture and drainage, agricultural production reduction, water management stress, and water scarcity. To prevent disasters and mitigate their effects, it is crucial to improve drought monitoring and research (Han et al. 2020; Yuce and Esit 2021). Effects of drought are influenced by variables including the deficiency of water level, the duration of the drought, and the size of the drought-affected area (Wilhite and Glantz 1985). In addition, extreme weather disasters (such as floods and droughts) and climate action have been listed as the two top high risks, which have had a significant impact on livelihoods, the environment, and society, according to the World Economic Forum (WEF) global risks report (WEF 2020).

Some authors have provided a thorough summary of the drought concept, its monitoring techniques, and the latest developments in trends (Wilhite 2000; Sheffield et al. 2004; Paulo and Pereira 2006; Mishra et al. 2010; Şen 2012, 2017; Wang et al. 2017; Şen et al. 2019). Meteorological drought:

✉ Musa Esit  
mesit@adiyaman.edu.tr

<sup>1</sup> Department of Civil Engineering, Adiyaman University, Adiyaman, Turkey

<sup>2</sup> Department of Civil Engineering, Dicle University, Diyarbakir, Turkey

This results from a lack of precipitation. In addition, it gives more knowledge on the level of dryness at a specific time. Hydrological drought: It refers to the impact of a period of low rainfall on the availability of water (surface or sub-surface) (Abro et al. 2022). A meteorological drought that lasts for several months causes soil drought to develop first, which results in crop loss, and then the drought develops into an agricultural drought. Agricultural drought, a result of a persistent meteorological drought, most severely impacts agro-based sectors (Abeyasingha et al. 2020). Response times are substantially slower in cases of hydrological drought (Lorenzo-Lacruz et al. 2013). The discrepancy in the timing of hydrological and meteorological droughts, whereby the hydrological drought typically occurs after the meteorological drought, is caused by the physical relationship between hydrological processes (Salimi et al. 2021).

The severity of the drought must be assessed using some type of index to conduct drought risk assessments and design mitigation plans. Numerous drought indices have been utilized to explain different types of droughts. A variety of data sets and complex computations are taken into account by the majority of meteorological and hydrological drought indices (Yeh 2019). In contrast, Streamflow Drought Index (SDI), the Standardized Precipitation Index (SPI), and Standardized Precipitation Evapotranspiration Index (SPEI) are useful indices that are simple to produce. SDI, proposed by Nalbantis (2008), defines the severity and characteristics of hydrological droughts. It can readily meet regional and application needs and can be applied on any timescale. Hence, the SDI has recently been used extensively in hydrological drought research (Malik et al. 2019, 2021; Jahangir and Yarahmadi 2020; Tareke and Awoke 2022). SPI, developed by McKee et al. (1993), is frequently used in research on meteorological droughts. It can successfully describe drought severity under various climatic circumstances and simply needs precipitation data. As a result, it has been applied to assess the characteristics of meteorological drought occurrences in many different regions and countries (Gidey et al. 2018; Sharafati et al. 2020; Bhunia et al. 2020; Dlamini et al. 2022). SPEI, developed by Vicente-Serrano et al. (2010), is a standardized drought index considering the water balance model and is widely used in drought assessment and monitoring in different climate conditions (Danandeh Mehr et al. 2020; Cao et al. 2022).

To assess and describe the drought conditions within a specific period, drought indices are frequently utilized (Tang et al. 2021; Ding et al. 2021; Ma et al. 2021; Zhang et al. 2022). In a study of regional meteorological and hydrological drought characteristics in Denmark, Hisdal and Tallaksen (2003) found that streamflow droughts are less common, less uniform across the region, and last longer than precipitation droughts. Khalili et al. (2011) used the SPI and the Reconnaissance Drought Index (RDI) in several climate zones in

Iran. According to their findings, the RDI can be particularly sensitive to climate fluctuation using potential evapotranspiration (ET<sub>0</sub>). In Greece, Tigkas et al. (2012) utilized the RDI and SDI; they evaluated regression equations between the two, which allowed them to predict the severity of the hydrological drought in real time for the whole year. Yuce et al. (2023) investigated the hydrological drought condition over Yeşilirmak basin, Türkiye using SDI index and ITA method. Mohammed et al. (2022) assessed the impact of agricultural drought considering SPI and SPEI indices on maize and wheat yield across Hungary. In recent studies, graphical trend methodologies are applied in the literature (Gumus et al. 2021; Katipoğlu 2022; Katipoğlu and Acar 2022; Chang and Niu 2023). For example, Elouissi et al. (2021) investigated drought events and trend by SPI and ITA methodology in Macta watershed. Alam et al. (2023) noted that spatio-temporal variability of meteorological drought considering SPI and ITA methods in the Luni River Basin, India.

Only a limited number of studies have combined the various individual indices, particularly those aimed at assessing meteorological and hydrological droughts, to obtain more thorough results from integrated assessments, despite a large number of studies on meteorological, hydrological, and agricultural droughts. For example, Edossa et al. (2010) discovered that hydrological droughts typically occurred seven months after meteorological droughts. Tabrizi et al. (2010) reported that meteorological drought observations at the annual time scale can be used to analyze the streamflow drought. Cheraghalizadeh et al. (2018) found the link between meteorological and hydrological droughts upstream and downstream of the Kasilian basin has been modeled using a copula-based joint meteorological-hydrological drought index. Wu et al. (2017) developed the non-linear model between meteorological and hydrological drought indices. Wang et al. (2020) investigated a comprehensive evaluation of hydrological drought and its relationships with meteorological drought in the Yellow River basin, in China. The phase angle correlations showed that meteorological drought in the YRB occurred earlier than hydrological drought, and the cross wavelet transforms demonstrated a positive relationship between hydrological and meteorological drought. Yılmaz et al. (2022) reported the effect of climate change on hydrological and meteorological droughts in the Coruh basin, Turkey. Bayer Altin and Altin (2021) investigated the response of hydrological drought to meteorological drought in the eastern Mediterranean basin of Turkey. Lin et al. (2023) studied on the propagation from meteorological to hydrological drought in the Xijiang River Basin, South China. Meresa et al. (2023) investigated the understanding the role of catchment and climate characteristics in the propagation of meteorological to hydrological drought. According to results, with increased aggregation

time, the probability of meteorological to hydrological drought propagated increases. The influence of watershed and climate controls on the severity of hydrometeorological drought varies by catchment.

This study assesses spatiotemporal characteristics of meteorological and hydrological drought trends of the lower Tigris-Euphrates basin (LTEB), Türkiye using SPI, SPEI, and SDI indices. It is one of the most important basins due to irrigation, agriculture and hydropower utilities. While being one of the Türkiye's most significant basins, LTEB has not been thoroughly investigated in terms of meteorological and hydrological droughts. First, a comprehensive dry and wet period at 12 months (annual) is investigated and compared by three indices. Second, meteorological and hydrological drought trends are evaluated by Mann–Kendall (MK), Spearman Rho (SR), and innovative trend analysis (ITA) methodologies for each month. Finally, wavelet transform coherence (WTC) is utilized to explore the relationship between drought indices and identify the lag in the propagation process.

## Materials and methodology

### Study area

The Euphrates and Tigris rivers, which are the transboundary waters of Türkiye, converge within the borders of Iraq and flow into the Persian Gulf in Shattularap. The part of the Euphrates-Tigris basin within the borders of Türkiye is approximately 185,000 km<sup>2</sup> and includes the areas, where drinking, utility, energy, and irrigation water are most needed (Alivi et al. 2021). GAP, Türkiye's most important regional development project, covers nine provinces (Adıyaman, Batman, Diyarbakır, Gaziantep, Kilis, Mardin, Siirt, Şanlıurfa, and Şırnak) located in the Euphrates-Tigris basin and upper Mesopotamian plains. It should be noted that the basin has a diversity of climatic characteristics in terms of its climatic conditions. The GAP region, which is constituted of broad plains in the lower Tigris-Euphrates basin, contains 20% of Türkiye's 8.5 million hectares of irrigable land. In the northern and eastern regions of the Euphrates-Tigris basin, the altitude reaches up to 4,000 m in mountainous areas. As it progresses toward the south of the basin, the topography changes rapidly and it is seen that relatively flat and plain areas dominate in these parts, where the altitude decreases to 300 m (Gumus et al. 2022).

In this paper, 11 hydrological stations and 23 meteorological stations data are considered in the study area (Fig. 1). Data on monthly precipitation and streamflow are gathered from the Turkish State Hydraulic Works and State Meteorological Service, respectively. The geographic details and record lengths of the hydrological and meteorological

stations used in this study are shown in Tables 1 and 2, respectively. According to Fig. 1, seven dams are constructed, namely, Kralkızı, Dicle, Devegeçidi, Ilısu, Atatürk, Birecik, Karakaya, and Keban dams in the study area. While the highest annual total mean precipitation is seen at the station as 803 mm, the lowest precipitation is observed at station 17,980 as 290.86 mm.

## Meteorological and hydrological drought assessment

### The standardized precipitation index (SPI)

The SPI was proposed by McKee et al. (1993). The World Meteorological Organization (WMO) advises using it globally because it is one of the indexes that may indicate the amount of precipitation in a specific period (Pei et al. 2019). The specific mathematical procedure is as follows:

If the amount of precipitation over a certain period is  $x$ , the distribution of the probability density function  $\Gamma$  is as follows:

$$f(x) = \frac{1}{\beta^\alpha \Gamma(\alpha)} x^{\alpha-1} e^{-\frac{x}{\beta}} \text{ for } x > 0 \tag{1}$$

where  $\beta$  and  $\alpha$  are the scale and shape parameters of  $\Gamma$  distribution function. For the precipitation  $x_0$  in a specific year, it is possible to determine the probability that the random variable  $x$  is smaller than  $x_0$ :

$$F(x < x_0) = \int_0^\infty f(x) dx \tag{2}$$

$$F(x = 0) = \frac{m}{n} \tag{3}$$

where  $n$  is the total number of samples and  $m$  is the number of samples with no precipitation. In the normalized normal distribution function, we substituted the probability value result:

$$F(x < x_0) = \frac{1}{\sqrt{2\pi}} \int_0^\infty e^{-\frac{x^2}{2}} dx \tag{4}$$

The solution to the formula above was as follows:

$$SPI = S \frac{t - (c_2 t + c_1) + c_0}{[(d_3 t + d_2) t + d_1] t + 1} \tag{5}$$

where

$$t = \sqrt{\ln \frac{1}{F^2}}$$

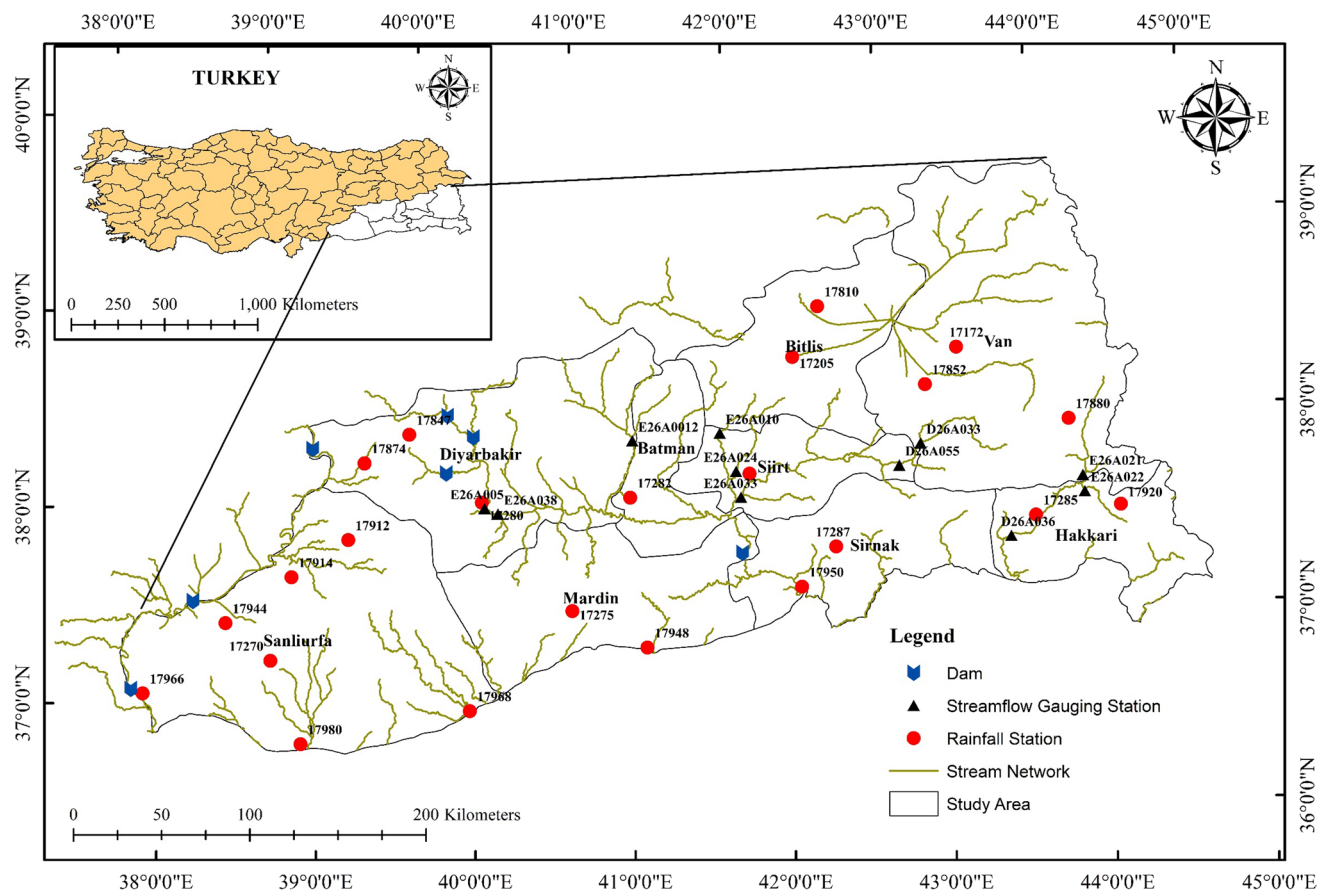


Fig. 1 Geographical location of streamflow and rainfall stations used in the study area

$$c_0 = 2.515517, c_1 = 0.802853, c_2 = 0.010328 \tag{6}$$

$$d_1 = 1.432788, d_2 = 0.189269, d_3 = 0.001308$$

where  $S$  is the coefficient for the probability density plus or minus,  $c_0, c_1, c_2$  and  $d_1, d_2, d_3$  are calculated parameters. If  $F > 0.5$ , then  $S = 1$ ; if  $F \leq 0.5$ , then  $S = -1$ .

**The standardized precipitation evapotranspiration index (SPEI)**

The Standard Precipitation Evaporation Index (SPEI), which was introduced by Vicente-Serrano et al. (2010), is one of the most widely used drought monitoring and tracking. This is mostly because, with the exception of SPI, which just requires data on precipitation, it depends on temperature and precipitation data. The "climatic water balance," which utilizes rainfall and potential evapotranspiration (PET) (Vicente-Serrano et al. 2010). SPEI depicts various forms of droughts over a variety of time scales, from 1 to 24 months. The climate-water balance was calculated using the formula below:

$$D_i = P_i - PET_i \tag{7}$$

where  $PET_i$  is potential evapotranspiration (mm) at month  $i$ ,  $P_i$  is precipitation (mm), and  $D_i$  is the moisture deficit (mm) at month  $i$ . In this study, the PET was calculated using the Thornthwaite method. For this procedure, only the average monthly air temperature and average daily daylight hours are required, and they may be calculated from latitude. The  $D_i$  values were summarized as follows at various time scales:

$$D_i^k = \sum_{i=0}^{k-1} (P_{n-1} - PET_{n-1}) \tag{8}$$

where  $k$  is the monthly time scale and  $n$  is the number of calculations.

**The standardized streamflow index (SDI)**

"Hydrological drought" refers to a lack of water and groundwater resources in the form of lake and reservoir water, the river flows, and groundwater levels (Tabari et al. 2013; Akbari et al. 2015; Malik et al. 2019). In this work, the hydrological drought is analyzed using the standardized streamflow index

**Table 1** Statistical characteristic and geographical location information of meteorological stations

Province	Station code	Latitude	Longitude	Period	Mean (mm)	SD	Cv	Cs	r
Van	17172	38.4693	43.346	1963–2021	397.022	74.229	0.18697	0.03144	1.01094
Van	17,880	38.0435	44.0173	1963–2021	432.195	106.185	0.24569	0.68038	1.00347
Van	17852	38.2963	43.1197	1982–2021	527.348	125.311	0.23763	0.32015	1.01456
Bitlis	17205	38.5033	42.2808	1964–2021	803.686	181.896	0.22633	-0.20046	1.00868
Bitlis	17810	38.7487	42.475	1964–2021	533.467	130.864	0.24531	0.19191	1.00038
Siirt	17210	37.9319	41.9354	1963–2021	703.563	173.605	0.24675	0.63330	1.02051
Şanlıurfa	17270	37.1608	38.7863	1963–2021	461.186	153.105	0.33198	0.70243	1.01895
Şanlıurfa	17912	37.7522	39.3291	1963–2021	563.724	151.581	0.26889	0.34898	1.00948
Şanlıurfa	17914	37.5806	38.9508	1967–2021	443.703	136.561	0.30778	0.83516	1.04382
Şanlıurfa	17944	37.3651	38.5134	1999–2021	390.883	113.356	0.28991	0.26655	1.01927
Şanlıurfa	17966	37.0281	37.9638	1964–2021	366.324	103.213	0.28175	0.47876	1.00869
Şanlıurfa	17968	36.8406	40.0307	1963–2021	304.202	108.595	0.35698	0.30556	1.02138
Şanlıurfa	17980	36.7276	38.9473	1965–2021	290.860	106.259	0.36533	1.19062	1.01398
Mardin	17275	37.3103	40.7284	1963–2021	671.032	221.940	0.33074	0.36929	1.01855
Mardin	17948	37.0945	41.18635	1966–2021	438.822	142.395	0.32449	0.22872	1.01333
Batman	17282	37.8636	41.1562	1963–2021	497.505	132.231	0.26579	0.42932	1.02054
Hakkari	17285	37.5745	43.7388	1963–2021	791.347	178.360	0.22539	0.67679	1.01695
Hakkari	17920	37.5785	44.2862	1964–2021	748.298	176.581	0.23598	0.53101	1.00414
Şırnak	17287	37.52028	42.445	1970–2021	710.738	171.178	0.24084	0.76609	1.00407
Şırnak	17950	37.3326	42.2027	1963–2021	686.554	198.142	0.28860	0.32931	1.02385
Diyarbakır	17847	38.267	39.766	1963–2021	745.834	192.093	0.25755	0.62721	1.00986
Diyarbakır	17874	38.1371	39.4644	1972–2021	739.224	212.378	0.28730	0.23888	1.00785
Diyarbakır	17280	37.8973	40.2027	1963–2021	496.251	128.309	0.25856	0.15782	1.01741

Mean annual total mean precipitation, SD standard deviation, Cv coefficient of variance, Cs skewness, rI kurtosis

**Table 2** Geographical information of streamflow stations of used in the study area

Province	Station code	Altitude (m)	Latitude	Longitude	Period
Siirt	E26A010	910	38.150	41.767	1965–2021
Batman	E26A0012	597	38.150	41.200	1980–2021
Siirt	E26A024	530	37.950	41.850	1980–2021
ŞİİRT	E26A033	457	37.817	41.867	1997–2017
Diyarbakır	E26A005	570	37.867	40.217	1980–1997
Diyarbakır	E26A038	563	37.833	40.300	2007–2021
Van	D26A033	1438	38.000	43.050	2003–2021
Van	D26A055	1350	37.900	42.900	2000–2021
Van	E26A021	1725	37.750	44.067	1999–2021
Hakkari	E26A022	1694	37.667	44.067	2003–2021
Hakkari	D26A036	1042	37.483	43.567	1977–1991

(SDI) developed by Nalbantis and Tsakiris (2009), which applies a similar concept to the SPI. The SDI is calculated assuming a time series of monthly streamflow volumes  $Q_i, j$ , where  $i$  denotes the hydrological year and  $j$  denotes the month within that year ( $j = 1$  for October,  $j = 12$  for September).  $V_{i,k}$  is evaluated using the following equation suggested by Nalbantis (2008):

$$V_{i,j} = \sum_{j=1}^{3k} Q_{i,j} \quad i = 1, 2, \dots, j = 1, 2, \dots, 12, k = 1, 2, 3, 4 \quad (9)$$

where  $V_{i,k}$  indicates the cumulative streamflow volume for the  $i^{\text{th}}$  hydrological year and  $k^{\text{th}}$  reference period,  $k = 1$  for October–December,  $k = 2$  for October–March,  $k = 3$  for October–June, and  $k = 4$  for October–September. Considering  $V_{i,k}$ , the SDI may be determined as follows for each reference period  $k$  in the  $i^{\text{th}}$  hydrological year:

$$SDI_{i,k} = \frac{V_{i,k} - \bar{V}_k}{S_k} \quad i = 1, 2, \dots, k = 1, 2, 3, 4 \quad (10)$$

where  $S_k$  and  $\bar{V}_k$  denote as the standard deviation and mean of the cumulative streamflow volumes of the reference period and  $V_k$  is utilized as the truncation level (Nalbantis

and Tsakiris 2009). Wetness/dryness categories based on employed three indices are given in Table 3.

### Methodologies of drought trends and relationships between hydrological and meteorological drought indices

#### Serial correlation analysis

The series correlation structure in a dependent time series will have an impact on Mann–Kendall's (MK) performance. More specifically, the presence of a positive series correlation in time series increases the probability of identifying a significant trend (Farris et al. 2021; Pang and Wang 2021). Therefore, the serial correlation structure of the series should be investigated before performing the MK test. If there is a significant series correlation in a data series, the test statistics should be reassessed or a preliminary method should be employed to reduce its impact. Hence, The trend-free pre-whitening approach (TFPW) is used in this study (Yue et al. 2002b). The first autocorrelation coefficient ( $r_1$ ) is calculated using the following formula:

$$r_k = \frac{\sum_{i=1}^{n-k} [(x_i - \bar{x})(x_{i+k} - \bar{x})]}{\sum_{i=1}^n (x_i - \bar{x})^2} \text{ for } i = 1 \rightarrow r_1, |r_1| > \frac{z_{\alpha/2}}{\sqrt{n}} \tag{11}$$

where  $x_i$  and  $\bar{x}$  are the serial values and the series mean, respectively, and  $n$  is the number of observations,  $k$  is the number of shifts. There is a series of internal dependency that needs to be eliminated if  $|r_1| > 1.96/\sqrt{N}$  according to a 95% confidence level.

#### Mann–Kendall (MK) and Spearman Rho (SR) tests

MK, the non-parametric test, described by Kendall (1975) is employed globally to find trends in hydrological and meteorological data. In this methodology, the test statistic  $S$  is calculated as

$$S = \sum_{k=1}^{n-1} \sum_{j=k+1}^n \text{sgn}(x_j - x_k) \tag{12}$$

where  $n$  represents a number of the data,  $x_j$  and  $x_k$  donate the data point in years  $j$  and  $k$  ( $j > k$ ) and  $t_i$  is the length of the tied rank group:

$$\text{sgn}(x_j - x_k) = \begin{cases} 1 & (x_j - x_k) > 0 \\ 0 & (x_j - x_k) = 0 \\ -1 & (x_j - x_k) < 0 \end{cases} \tag{13}$$

$$\text{Var}(S) = \frac{n(n-1)(2n+5) - \sum_i t_i(t_i-1)(2t_i+5)}{18} \tag{14}$$

$$Z = \begin{cases} \frac{S-1}{\sqrt{\text{Var}(S)}} & S > 0 \\ 0 & S = 0 \\ \frac{S+1}{\sqrt{\text{Var}(S)}} & S < 0 \end{cases} \tag{15}$$

An upward trend is indicated by a positive  $Z$  number, whereas a downward trend is shown by a negative value. Critical test statistical values are 1.645, 1.96, and 2.57 at 90%, 95%, and 99% significant levels, respectively (Yuce and Esit 2021). Similar to the MK test, Spearman's Rho (SR) test determines the monotonic trend in the time series and is nonparametric. According to the  $H_0$  hypothesis, the series' data are uniform, which suggests that no trend can be seen in the data. The SR correlation coefficient ( $r_s$ ) and related test statistic ( $Z$ ) are defined as follows for the analysis of trends:

$$r_s = 1 - \frac{[6\sum_{i=1}^n (Rx_i - i)^2]}{n(n^2 - 1)} \tag{16}$$

$$z = r_s \sqrt{n-1} \tag{17}$$

The data are sorted to get the  $R_{x_i}$  (rank statistic), where  $n$  is the length of the time series. The null hypothesis of no trend is rejected for  $z > 1.645$  at the 10% level of significance (Yue et al. 2002a).

#### Innovative trend analysis (ITA) with significance test

Şen (2012) presented the ITA technique to find changes between the first and second halves of a time series. Each half must have an equal number of data points and be arranged in a particular order (either upward or downward). Data points from both halves are paired and plotted on a diagonal (1:1) line at a 45-degree angle in a Cartesian coordinate system. The X-axis and Y-axis show the data values for the first and second halves of the graph, respectively. The approach's founding principle is that two identical ranking pairs from the first and second halves should lie along a 1:1 line. According to Fig. 2, points

**Table 3** Drought classifications based on SPI, SDI, and SPEI values

Category	Criterion
Non-Drought	SPI, SPEI and SDI $\geq 0.0$
Mild drought	$-1.0 \geq$ SPI, SPEI and SDI $< 0.0$
Moderate drought	$-1.5 \geq$ SPI, SPEI and SDI $< -1$
Severe drought	$-2.0 \geq$ SPI, SPEI and SDI $< -1.5$
Extreme drought	SPI, SPEI and SDI $< -2.0$

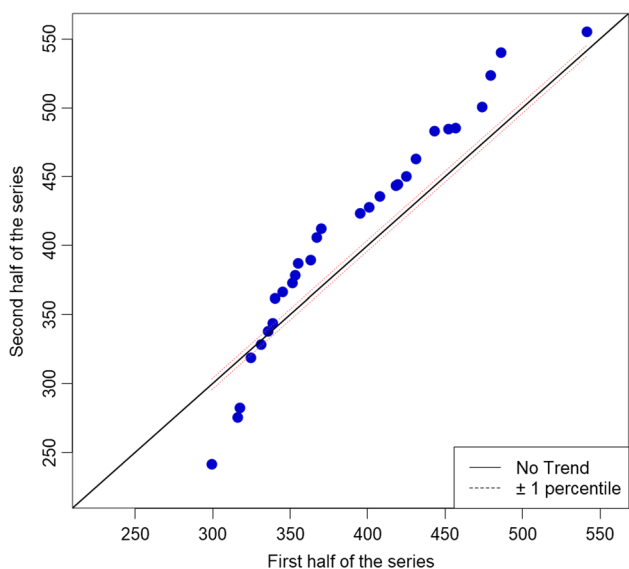


Fig. 2 Visualization of the ITA approach

show an increasing trend if they are above the 1:1 (45°) line, a decreasing trend if they are below the line, and no trend if they are on the line.

Sen (2017) introduces the statistical significance test. After splitting the hydrometeorological time series in half, this method calculates their arithmetic averages ( $y_1$  and  $y_2$ ). The following formula is used to calculate the trend slope ( $s$ ):

$$E(s) = \frac{2}{n} [E(\bar{y}_2) - E(\bar{y}_1)] \tag{18}$$

$$\sigma_s^2 = \frac{8}{n^2} [E(\bar{y}_2^2) - E(\bar{y}_2\bar{y}_1)] \tag{19}$$

$$\rho_{\bar{y}_2\bar{y}_1} = \frac{E(\bar{y}_2\bar{y}_1) - E(\bar{y}_2)E(\bar{y}_1)}{\sigma_{\bar{y}_2}\sigma_{\bar{y}_1}} \tag{20}$$

$$\sigma_s^2 = \frac{8}{n^2} \frac{\sigma^2}{n} (1 - \rho_{\bar{y}_2\bar{y}_1}) \tag{21}$$

$$\sigma_s = \frac{2\sqrt{2}}{n\sqrt{n}} \sigma \sqrt{(1 - \rho_{\bar{y}_2\bar{y}_1})} \tag{22}$$

where  $E(s)$  is the first-order moment of the slope,  $n$  denotes the length of the data, and  $\rho$  means the cross-correlation coefficient between two sections,  $\sigma_s^2$  shows the trend slope variance, and  $\sigma_s$  is the trend slope standard deviation. The following formula is used to calculate the trend slope's confidence interval:

$$CL_{(1-\alpha)} = 0 \pm s_{cri}\sigma_s \tag{23}$$

$s_{cri}$  is the value of  $z$  that was determined using a certain level of confidence from the standard normal distribution. The trend is considered to be increasing (decreasing) if the trend slope exceeds the higher (lower) confidence level. There is no statistically significant trend if these requirements are not met at a specific level of confidence.

### Wavelet transform coherence (WTC)

WTC is used to assess the cross-wavelet transform's coherence between time series in a time frequency. Numerous disciplines have adopted the common variation zone of two-time series in the time–frequency space (Torrence and Webster 1999). The following equation is a description of the WTC of two signals:

$$R_n^2(s) = \frac{|S(s^{-1}W_n^{XY}(s))|^2}{S(s^{-1}|W_n^X(s)|^2)S(s^{-1}|W_n^Y(s)|^2)} \tag{24}$$

where  $W_n^{XY}$  presents the cross-wavelet transform and  $S$  donates a smoothing operator defined as follows:

$$S(W) = S_{scale}(S_{time}(W(s))) \tag{25}$$

where  $S_{scale}$  and  $S_{time}$  show wavelet time translation axis and smoothing along the wavelet telescopic scale axis, respectively. Equations (26) and (27) employ a suitable smoothing operator for the Morlet wavelet, in which  $\Pi$  displays the rectangle function,  $c_1$  and  $c_2$  indicate normalized constants, and the scale de-correlation length for the Morlet wavelet is derived empirically to be 0.6 (Grinsted et al. 2004). An exact definition of a Morlet wavelet's smoothing operator is

$$S_{time}(W)|_s = \left( W_n(s)c_1^{-\frac{t^2}{2s^2}} \right) |_s \tag{26}$$

$$S_{scale}(W)|_s = (W_n(s)c_2\Pi(0.6s))|_s \tag{27}$$

## Results

### Serial correlation in meteorological and hydrological drought indices

The  $r_1$  values at lag-1 for meteorological drought indices (SPI and SPEI) and hydrological drought indices (SDI) are investigated. The crucial points of the  $r_1$  lie between 0.2 and 0.4 considering SPI/SPEI values and range from 0.2 to 0.6 for SDI values. Any value outside of this range indicates

that the series has a serial correlation. The significant serial correlation at lag-1 is 20/49 months (7.24%/17.25%) for SPI/SPEI. In addition, the significant serial correlation at lag-1 is 5 months (3.78%) for SDI in Table 4. In general, station 17,810 demonstrates a serial correlation in all months (except August and September) based on SPI and SPEI indices. Furthermore, SPEI captures more serial dependence than SPI. However, the serial correlation dependence captured by the SPI drought index is also observed by the SPEI drought index. This study used the trend-free pre-whitening (TFPW) methodology to eliminate the intrinsic dependence on drought indices (SPI, SPEI, and SDI). Following that, the M–K test is performed using the new series, which lacks serial correlation.

### Examination of the monthly trends in the hydrological and meteorological drought

Figure 3 indicates the monthly meteorological (SPI and SPEI) and hydrological drought (SDI) results using MK and SR tests at a 12-month time scale. According to SPI results, stations 17275, 17810, 17948, 17847, 17874, 17950, and 17968 for almost all months display decreasing trend in dry categories based on MK test results at the 95% significant levels ( $\pm 1.96$ ). While an increasing trend implies no drought, a decreasing trend in the indices for the dry categories indicates the presence of drought. Therefore, these stations have significantly increased drought occurrences in the dry categories. Station 17270 in March, and April and station 17980 in April and December indicate a significantly decreasing trend at the 12-month time scale. SR test results reveal consistency with the result of the MK test. However, MK test results show more sensitivity than SR test results

in dry categories. For example, MK and SR tests result at station 17270 in April captured -2.13 and -1.74, respectively. Therefore, a decreasing trend is observed at some stations by the MK test, while the same trends aren't detected by the SR test. In general, SR test results show a lower trend at significant levels compared to the MK test.

When considering SPEI drought indices, a decreasing trend is detected at stations 17270, 17275, 17810, 17847, 17874, 17880, 17948, 17950, 17966, 17968, and 17980 for all months at a 95% significant level. In addition, station 17172 (except July and August), 17205 in December (MK) station 17210 (Jan-May, September (MK) and December), and station 17285 (except February and November (MK)) are also significantly decreasing trends observed. These results indicate that SPEI drought indices detect a much more decreasing trend compared to SPI indices. Therefore, SPEI is more sensitive than SPI based on both trend tests. According to both meteorological drought assessments, most of the stations have under drought risk categories due to trend analysis results. According to SDI indices, no significant trend is detected at the 12-month time scale for all stations.

Figure 4 indicates monthly meteorological and hydrological drought trends based on the ITA method at stations 17275 (a-) SPI and b-) SPEI) and E26A010 (c-) SDI) as an example. The black line displays the trend slope, while the red and green lines represent lower and upper limits, respectively. According to Fig. 4, decreasing trends are observed significantly at all months due to higher trend slopes.

Tables 5 and 6 show the meteorological and hydrological drought trends for all months and all stations at a 95% confidence level, respectively. Considering Table 5, SPI and SPEI drought trends illustrate not appropriate results.

**Table 4** Serial correlation coefficient at lag-1 for monthly SDI drought index

SDI													
Station	Jan	Feb	Mar	Apr	May	Jun	Jul	Aug	Sep	Oct	Nov	Dec	Critical Value ( $\alpha=0.05$ )
D26A033	0.022	0.033	0.05	0.133	0.173	0.03	-0.026	-0.056	-0.072	-0.068	-0.059	-0.054	0.450
D26A036	0.051	0.056	0.048	0.331	0.476	0.341	0.206	0.13	0.097	0.067	0.04	0.042	0.506
D26A055	-0.067	-0.028	-0.031	0.103	0.214	0.072	-0.003	-0.042	-0.065	-0.071	-0.093	-0.062	0.418
E26A005	0.21	0.315	0.22	0.001	-0.153	-0.186	-0.196	-0.203	-0.208	-0.223	-0.127	0.134	0.462
E26A010	<b>0.272</b>	<b>0.274</b>	<b>0.288</b>	<b>0.337</b>	0.15	0.089	0.071	0.064	0.058	0.059	0.129	0.248	0.260
E26A012	0.151	0.235	0.219	0.085	-0.141	-0.218	-0.22	-0.226	-0.231	-0.206	-0.093	0.082	0.409
E26A021	0.04	0.04	0.041	0.123	0.281	0.175	0.097	0.065	0.055	0.05	0.047	0.043	0.450
E26A022	0.064	0.069	0.061	0.265	0.15	0.063	0.018	0.008	-0.005	0.001	0.008	0.067	0.506
E26A024	0.212	0.281	<b>0.31</b>	0.253	0.126	0.074	0.053	0.04	0.032	0.031	0.086	0.188	0.302
E26A033	0.32	0.308	0.221	0.355	0.397	0.351	0.336	0.331	0.328	0.337	0.343	0.343	0.400
E26A038	0.037	-0.002	0.077	-0.024	-0.104	-0.15	-0.153	-0.188	-0.176	-0.164	-0.151	-0.023	0.524

Bold values represent significant at  $\alpha = 0.05$  level



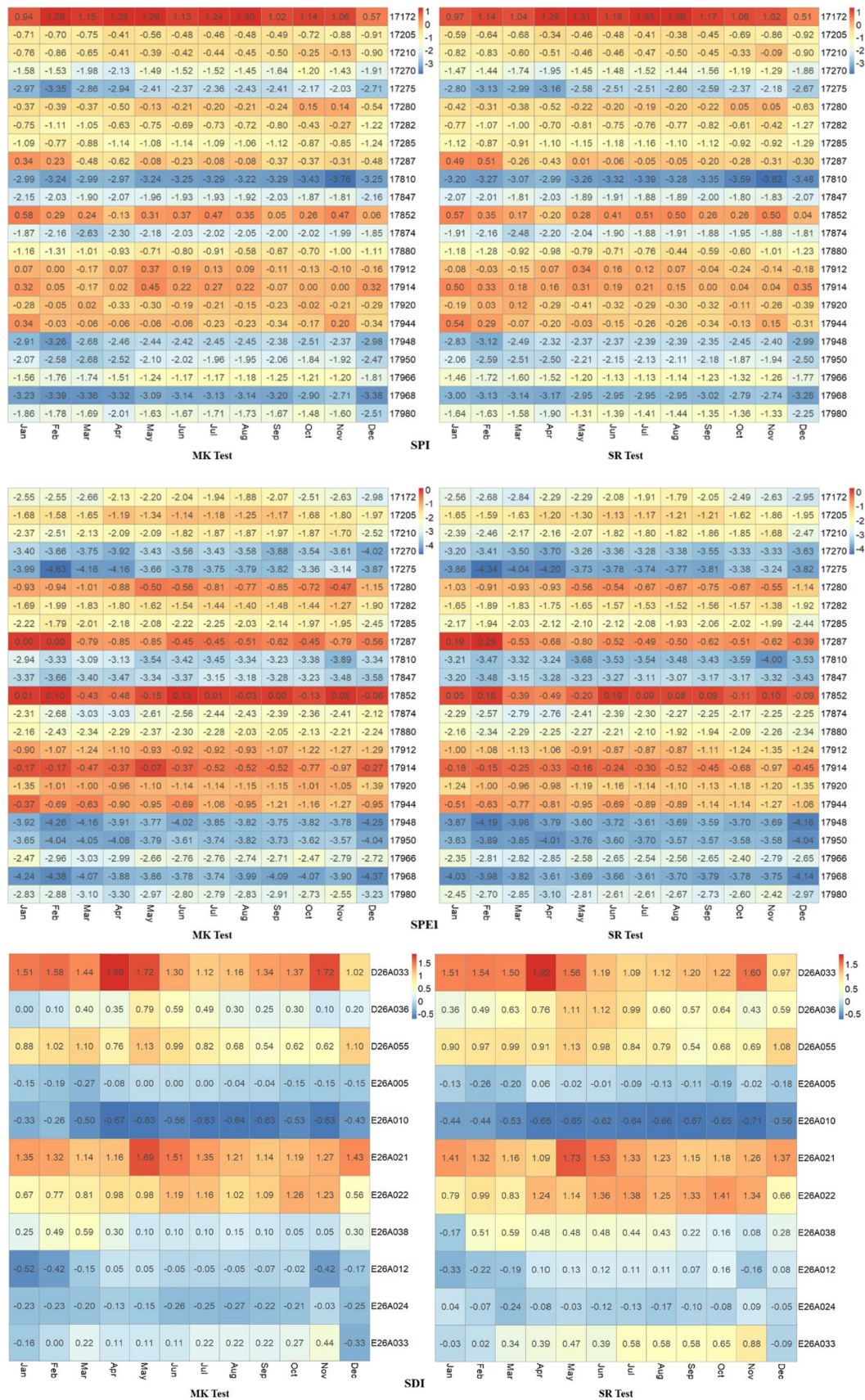
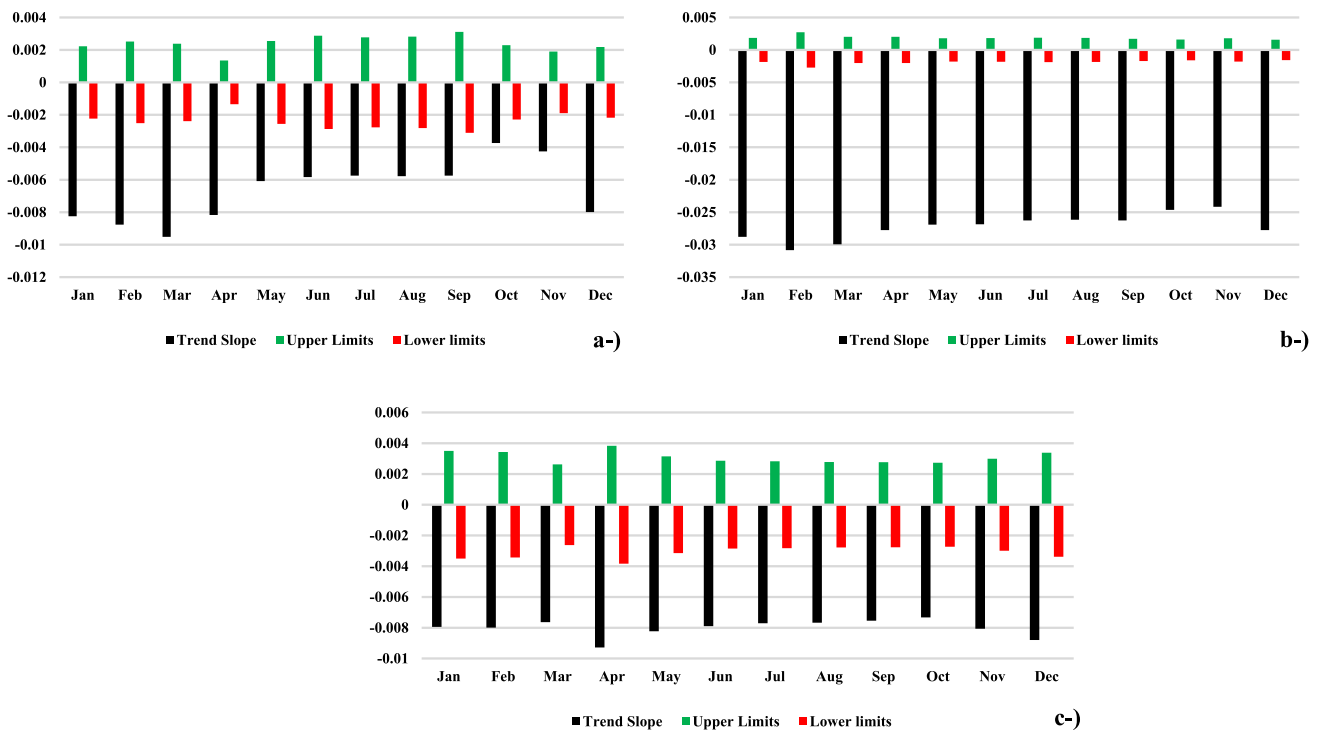


Fig. 3 Monthly meteorological and hydrological drought trends considering MK and SR tests based on 12-month time scale



**Fig. 4** Monthly meteorological and hydrological drought trends considering the ITA method based on the 12-month time scale; **a** station 17275 for SPI, **b** station 17275 for SPEI, and **c** station E26A010 for SDI

**Table 5** Monthly meteorological drought trend using the ITA method

SPI/SPEI		Jan	Feb	Mar	Apr	May	Jun	Jul	Aug	Sep	Oct	Nov	Dec
Station no	17172	↑/↓	↑/↓	↑/↓	↑/↓	↑/↓	↑/↓	↑/↓	↑/↓	↑/↓	↑/↓	↑/↓	↑/↓
	17205	↓/↓	↓/↓	↓/↓	↓/↓	↓/↓	↓/↓	↓/↓	↓/↓	↓/↓	↓/↓	↓/↓	↓/↓
	17210	-/↓	-/↓	-/↓	-/↓	-/↓	-/↓	-/↓	-/↓	-/↓	-/↓	-/↓	↓/↓
	17270	↓/↓	↓/↓	↓/↓	↓/↓	↓/↓	↓/↓	↓/↓	↓/↓	↓/↓	↓/↓	↓/↓	↓/↓
	17275	↓/↓	↓/↓	↓/↓	↓/↓	↓/↓	↓/↓	↓/↓	↓/↓	↓/↓	↓/↓	↓/↓	↓/↓
	17280	-/↓	-/↓	-/↓	-/↓	-/-	-/-	-/-	-/-	-/↓	↑/↓	↑/↓	-/↓
	17282	↓/↓	-/↓	↓/↓	-/↓	-/↓	-/↓	-/↓	-/↓	-/↓	-/↓	-/↓	↓/↓
	17285	↓/↓	↓/↓	↓/↓	↓/↓	↓/↓	↓/↓	↓/↓	↓/↓	↓/↓	-/↓	↓/↓	↓/↓
	17287	-/-	↑/-	↑/↓	-/-	-/↓	-/-	-/-	-/-	-/-	-/-	-/-	↑/-
	17810	↓/↓	↓/↓	↓/↓	↓/↓	↓/↓	↓/↓	↓/↓	↓/↓	↓/↓	↓/↓	↓/↓	↓/↓
	17847	↓/↓	↓/↓	↓/↓	↓/↓	↓/↓	↓/↓	↓/↓	↓/↓	↓/↓	↓/↓	↓/↓	↓/↓
	17852	↑/↑	↑/↑	↑/↑	↑/↑	↑/↑	↑/↑	↑/↑	↑/↑	↑/↑	↑/↑	↑/↑	↑/↑
	17874	↓/↓	↓/↓	↓/↓	↓/↓	↓/↓	↓/↓	↓/↓	↓/↓	↓/↓	↓/↓	↓/↓	↓/↓
	17880	-/↓	-/↓	-/↓	-/↓	-/↓	-/↓	-/↓	-/↓	-/↓	-/↓	-/↓	-/↓
	17912	↑/↓	↑/↓	↑/↓	↑/↓	↑/↓	-/↓	-/↓	↑/↓	↑/↓	↑/↓	↑/↓	-/↓
	17914	↑/-	↑/-	↑/-	↑/-	↑/-	↑/-	↑/-	↑/-	-/↓	-/↓	↑/↓	-/↓
	17920	↑/↓	↑/↓	↑/↓	↑/↓	↑/↓	↑/↓	↑/↓	↑/↓	↑/↓	↑/↓	↑/↓	↑/↓
	17944	↑/-	↑/-	↑/-	↑/-	↑/-	↑/-	↑/-	↑/-	↑/↓	↑/↓	↑/↓	↑/↓
	17948	↓/↓	↓/↓	↓/↓	↓/↓	↓/↓	↓/↓	↓/↓	↓/↓	↓/↓	↓/↓	↓/↓	↓/↓
	17950	↓/↓	↓/↓	↓/↓	↓/↓	↓/↓	↓/↓	↓/↓	↓/↓	↓/↓	↓/↓	↓/↓	↓/↓
	17966	↓/↓	↓/↓	↓/↓	↓/↓	↓/↓	↓/↓	↓/↓	↓/↓	↓/↓	↓/↓	↓/↓	↓/↓
	17968	↓/↓	↓/↓	↓/↓	↓/↓	↓/↓	↓/↓	↓/↓	↓/↓	↓/↓	↓/↓	↓/↓	↓/↓
	17980	↓/↓	↓/↓	↓/↓	↓/↓	↓/↓	↓/↓	↓/↓	↓/↓	↓/↓	↓/↓	↓/↓	↓/↓

↑ increasing, ↓ decreasing, - no trend

**Table 6** Monthly hydrological drought trend using the ITA method

SDI												
Station no	Jan	Feb	Mar	Apr	May	Jun	Jul	Aug	Sep	Oct	Nov	Dec
D26A033	↑	↑	↑	↑	↑	↑	↑	↑	↑	↑	↑	↑
D26A036	↑	↑	↑	↑	↑	↑	↑	↑	↑	↑	↑	↑
D26A055	↑	↑	↑	↑	↑	↑	↑	↑	↑	↑	↑	↑
E26A005	↓	↓	↓	↓	↓	↓	↓	↓	↓	↓	↓	↓
E26A010	↓	↓	↓	↓	↓	↓	↓	↓	↓	↓	↓	↓
E26A021	↑	↑	↑	↑	↑	↑	↑	↑	↑	↑	↑	↑
E26A022	↑	↑	↑	↑	↑	↑	↑	↑	↑	↑	↑	↑
E26A038	–	–	↓	↓	↓	↓	↓	↓	↓	↓	↓	↓
E26A012	–	–	↓	↓	–	–	–	–	–	–	–	–
E26A024	↓	↓	↓	↓	↓	↓	↓	↓	↓	↓	↓	↓
E26A033	↑	↑	↑	↑	↑	–	–	–	–	–	–	–

↑ increasing, ↓ decreasing, – no trend

For example, increasing trends are detected by SPI indices for all months whereas decreasing trends are captured by SPEI indices at stations 17172, 17912, and 17920. However, the trend results of the two indices are in parallel at stations 17205 (↓), 17270 (↓), 17275 (↓), 17282 (↓), 17285 (↓), 17810 (↓), 17847 (↓), 17852 (↑), 17874 (↓), 17948 (↓), 17950 (↓), 17966 (↓), 17968 (↓) and 17980 (↓). In addition, both indices detect no trends (-) at stations 17280 (May, Jun, July, and August) and 17287 (April, Jun, July, August, September, October, and November).

Table 6 shows that, in contrast to MK and SR tests, the results of the hydrological drought trend using the ITA approach show a significant difference. Because, stations D26A033, D26A036, D26A055, E26A021, E26A022, and E26A033 (January, February, March, April, and May) tend to increase trend (↑) for all months at 95% confidence level, while decreasing trends (↓) in hydrological drought are noted at stations E26A005, E26A010, E26A038 (except January and February) and E26A024. Furthermore, a few stations including E26A038 (January and February), E26A0012 (except March and April), and E26A033 (from June to December) show no trend (-) significantly.

**Comparison of trend tests based on drought indices**

Table 7 indicates MK, SR, and ITA results for monthly SPI values. ITA results display more detected trends at all stations compared to MK and SR tests. However, In the trends detected by the MK and SR tests, the ITA method is also in harmony with these trends. It can be inferred from Table 7 that the ITA method is more successive to finding the hidden trend in the time series rather than other tests. For example, while MK and SR test captures significantly no trend at station 17172, the ITA test demonstrates an increasing trend for all months at a 95% confidence level. In addition, the ITA method detects a significantly decreasing trend at

station 17205, whereas no trends are observed by MK and SR tests. But all trend test results are in parallel at stations 17275, 17810, 17948, 17950, and 17968 which are decreasing trends for all months. Interestingly, increasing trends are only observed by the ITA method at stations 17912, 17914, 17920, and 17944, while MK and SR tests show no significantly captured trend.

Table 8 displays a comparison of trend tests for monthly SPEI values. According to Table 7, SPEI is a more sensitive detected trend rather than SPI considering all trend tests. For instance, no trends are observed for station 17172 by MK and SR tests according to SPI, while a decreasing trend is significantly captured by SPEI. When all stations are taken into account, the ITA method detects an increasing trend at station 17852, although other tests show no apparent trend. The three trend tests are found to be more consistent with each other when compared to the SPI. Because, in comparison to SPI, there are more decreasing trends in stations. In particular, these stations are 17172, 17270, 17275, 17810, 17847, 17880, 17948, 17950, 17966, 17968, and 17980. Table 9 reveals the comparison of trend test results of SDI values. The ITA method, as opposed to the other two methods, is clearly more effective at identifying hidden trends. For example, no significant trends are observed at all employed stations according to MK and SR tests, while the ITA method captures significantly increasing/decreasing trends except stations E26A038 (January and February), E26A012 (January, February, and from May to December) and E26A033 (from June to December).

**Correlation analysis between meteorological and hydrological drought indices**

Figure 5 shows the variation in SPI–SPEI/SDI values across the chosen stations. Stations on the basin that are close to each other are chosen. Therefore, the relationship



**Table 9** Comparison of MK, SR, and ITA test results for monthly SDI values

Station No	Jan			Feb			Mar			Apr			May			Jun			Jul			Aug			Sep			Oct			Nov			Dec					
	MK	SR	ITA	MK	SR	ITA	MK	SR	ITA	MK	SR	ITA	MK	SR	ITA	MK	SR	ITA	MK	SR	ITA	MK	SR	ITA	MK	SR	ITA	MK	SR	ITA	MK	SR	ITA	MK	SR	ITA			
D26A033																																							
D26A036																																							
D26A055																																							
E26A005																																							
E26A010																																							
E26A021																																							
E26A022																																							
E26A038																																							
E26A012																																							
E26A024																																							
E26A033																																							
	Increasing			Decreasing			No Trend																																

between stations 17210-E26A024, 17210-E26A033, 17280-E26A005, 17280-E26A038, 17282-E26A012 and 17285-D26A036 are presented in Fig. 5. In addition, besides these stations, stations 17852-D26A055, 17880-E26A021, 17920-E26A021, and 17920-E26A022 are considered in this study. According to the relation between stations 17210-E26A024, SPEI captures the extreme droughts in the years of 2008 (April, May, and June). SDI displays the extreme drought in the years of 2008 (December) until 2009 (January and February) and the years 2000 (March, April, May, and December) until 2001 (January and February). In addition, the years 2000 (March) and 2008 (from April to September) are captured by SPI. According to extreme drought results, the hydrological drought began after a few months from the start of the extreme meteorological drought to its end. The results of relationships between stations 17210-E26A033 indicate that SPI/SPEI has a good agreement compared to SDI. However, the extreme drought category isn't seen at station E26A033. When considering the relation between stations 17280-E26A005, all used indices display that extreme droughts occur in the years of 1989. Furthermore, there is no extreme drought considering stations 17280 and E26A005. All results indicate that SPI is more sensitive than SPEI in terms of drought categories. For example, SPI detects extreme droughts in the years 1989 (from July to October) and 2000 (November), while SPEI doesn't detect the same extreme drought. In addition, extreme drought is observed by the SDI in the years 2001 (from March to December). it is clearly seen that the time between extreme meteorological drought and a hydrological drought was discovered to be 4 months. According to the relation between stations 17285-D26A036, SPI and SPEI indicate the same year (1989) for capturing extreme drought whereas SDI does not show any detected extreme drought. But SDI and SPI are consistent demonstrations in wet (> 2) categories rather than SPEI.

Table 10 indicates the correlation between meteorological and hydrological drought indices at a 12-month time

scale using the Pearson test. The highest correlation is found as 0.799 between stations 17210 and E26A024, while the lowest correlation is observed as 0.294 between 17852-D26A055 (SPEI-SDI). The differences between hydrological and meteorological indices are not particularly significant. For example, the correlations between SPI-SDI and SPEI-SDI are evaluated as 0.744 and 0.776 for stations 17210-E26A033, respectively.

In this section, the WTC analysis is utilized to assess the connections between the research area's monthly SPI/SPEI and SDI drought indices. The WTC is used to determine whether the selected drought indices exhibit any apparent oscillatory behavior. The results of the WTC analysis between the drought indices at 12-month periods are shown in Fig. 6. A relative phasing of the two-time series is displayed on each panel in this figure to demonstrate the causal relationships between the employed indices. Frequencies and times in the cold regions outside of the major areas (bluish regions) demonstrated no dependency on time. The causation between two-time series can be assessed using the phase patterns. The significance of arrow direction can be explained by the following: (1) when arrow directions move to the right, hydrological stations and meteorological stations are in phase (positively related); (2) when arrow directions move to the left, hydrological stations and meteorological stations are in anti-phase (negatively related); and (3) arrows pointing in different directions are used to indicate the leads or lags between two-time series. Arrow directions to the left up or right down, for instance, show that the hydrological station is leading, whereas arrow directions to the left down or right up show that the meteorological station is leading. The first and second variables in Fig. 6 correspond to meteorological and hydrological stations, respectively.

To achieve the most accurate understanding, only important areas of the WTC graph should be taken into account. Two meteorological indices exhibit the same manner

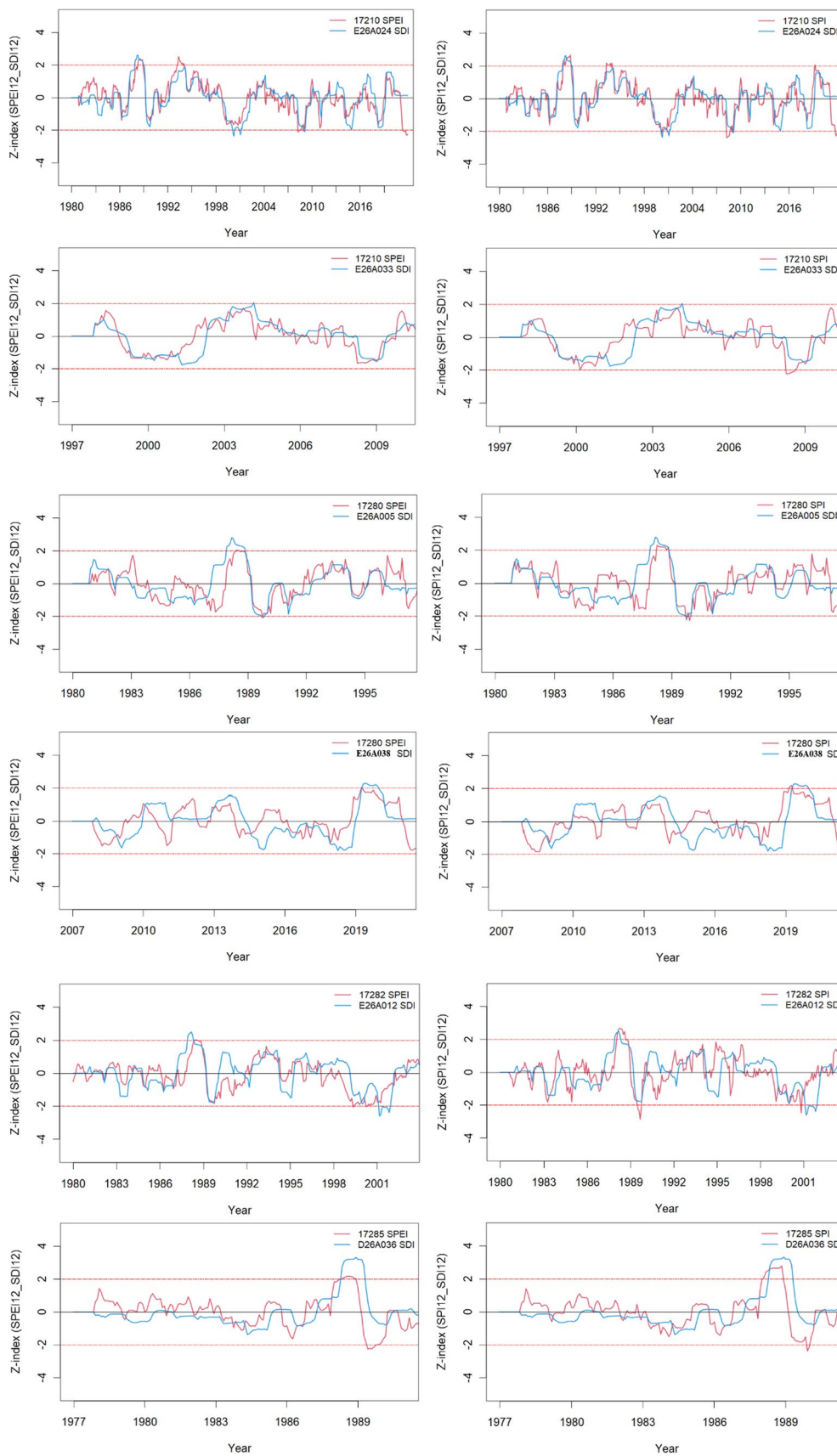


Fig. 5 Time series of drought indices for selected stations used to identify significant meteorological (SPEI-SPEI) and hydrological (SDI) droughts

**Table 10** Comparison between meteorological and hydrological indices considering Pearson correlation test

Indices/station	17210- E26A024	17210- E26A033	17280- E26A005	17280- E26A038	17282- E26A012	17285- D26A036	17852- D26A055	17880- E26A021	17920- E26A021	17920- E26A022
SPI12-SDI12	0.799	0.744	0.591	0.447	0.508	0.558	0.338	0.492	0.322	0.353
SPEI12-SDI12	0.775	0.776	0.636	0.476	0.644	0.471	0.294	0.472	0.307	0.305

with hydrological indices in Fig. 6. the WTC obtained for the DE26A024-17210 indicates some important positive period signals of 16–128 months during 1982–2016. In addition, a higher positive correlation is observed on the higher signals between meteorological and hydrological indices. When considered between stations E26A033 and 17210, the main significant positive period signals of 0–8 months during 2001–2004, 6–8 months from 2004 to 2006, and 0–5 months from 2007 to 2008. According to the relations between E26A005 and 17280, a good correlation is found both in lower and higher signals. The significant positive period of the signal was mainly concentrated in the cycle of 12–35 months in 1985–1995 and 4–10 months during 1984–1989. In addition, the relation between stations E26A038 and 17280, a positive correlation is mainly detected in the 0–8 month band from 2007 to 2011, 0–6 month from 2016 to 2019 and hydrological drought led to the meteorological drought. When considering stations E26A012-17282, At the 8–32-month band, positive period signals are captured in the years 1985–1997 and the 32–64 month band in 1983–1997. According to stations D26A036-17285, the significant positive period of signal mainly concentrated in the cycle of 16–35 months in 1979–1989.

WTC can more clearly show the connections and particular characteristics of oscillation periods that fluctuate with time, as well as the internal correlation between the hydrological and meteorological drought in the basin. Given that the onset of hydrological drought occurs somewhat later than that of meteorological drought. There is a strong correlation between the indices and it is possible that meteorological drought may accelerate the onset of hydrological drought. Due to arrow directions moving to the right-down, WTC of the monthly meteorological and hydrological stations shows that hydrological drought leads to meteorological drought for all in-phase (positively related) for all periods.

### Conclusions

Drought, one of the worst and most frequent natural disasters, has a negative impact on human life. In this paper, SPI/SPEI and SDI are chosen as the meteorological and hydrological drought indices, respectively. Investigation and comparison of the evaluation characteristics of hydrological and meteorological droughts are conducted. To assess monthly trends of the SPI/SPEI and SDI series, MK, SR, and ITA tests have been applied to all stations. Lower Tigris-Euphrates basin, Türkiye nearby meteorological and hydrological stations are chosen, and the Pearson Rho correlation test is computed at 12-month time scale. Finally, the links between hydrological and meteorological drought are explained in the

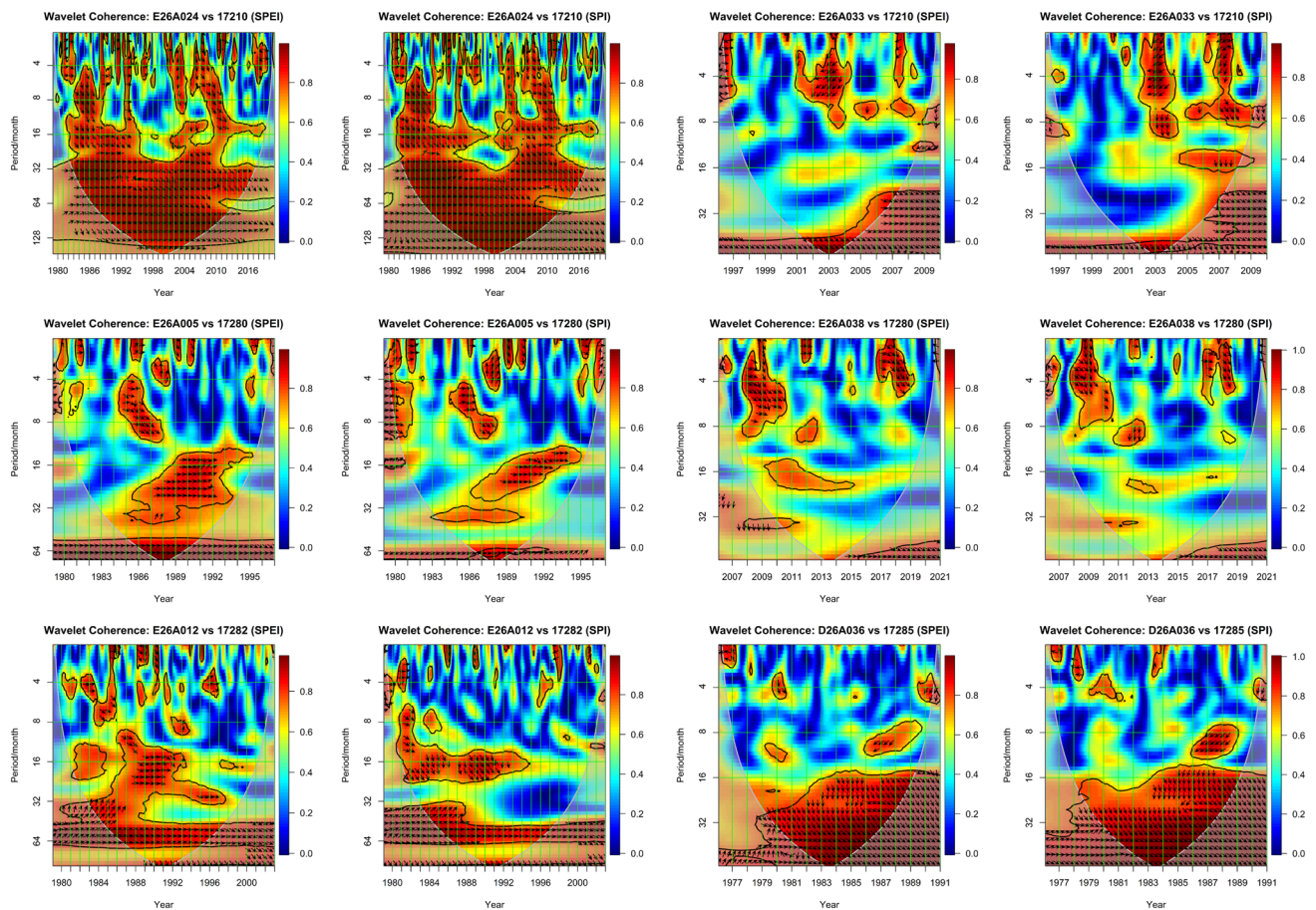


**Fig. 6** WTC analysis results between monthly SPI/SPEI and SDI drought indices at 12-month time scales. The arrows in the figures depict the phase difference of periods and coherence of more than 0.5

between two data series, and the thick enclosed regions indicate a statistical significance level of 5% versus a red noise process

basin utilizing the wavelet coherence approach. The following are key conclusions from the findings:

- A decreasing trend in the indices for the dry categories shows the existence of drought, whereas an upward trend implies the absence of drought. As a result, drought occurrences at the dry categories have increased significantly at stations 17275, 17810, 17948, 17847, 17874, 17950, and 17968 for almost all months at the 95% significant levels ( $\pm 1.96$ ) according to SPI. The results of the SR test are consistent with those of the MK test. However, in dry categories, MK test results are more sensitive than SR test results. In comparison to the MK test, the results of the SR test generally reveal a lower trend at significant levels. At stations 17270, 17275, 17810, 17847, 17874, 17880, 17948, 17950, 17966, 17968, and 17980, a decreasing trend is observed for all months when the SPEI drought indices are considered. These findings suggest that SPEI drought indices are substantially more sensitive to decreasing trends than

SPI indices. According to both trend tests, SPEI is more sensitive than SPI. Both meteorological drought assessments identify the majority of the stations under drought risk categories as a result of the findings of trend analysis. The 12-month time period for all stations does not show any obvious trend, according to SDI. Results of the hydrological drought trend using the ITA approach show a significant difference from MK and SR tests. Results are convenient with the previous studies (Achite et al. 2021; Akçay et al. 2022)

- ITA results display a more detected trend at all stations compared to MK and SR tests. However, in the trends identified by the MK and SR tests, the ITA approach is similarly in harmony with these trends. It can be concluded that the ITA method is more effective than other tests at detecting hidden trends in time series at a 95% confidence level. The findings of all trend tests conducted identically at stations 17275, 17810, 17948, 17950, and 17968 are significantly decreasing for all months considering SPI. Considering all trend tests, SPEI is more sensi-



tive in trend detection than SPI. In addition, When SPEI is compared to the SPI, the three trend tests are found to be more consistent with each another. According to SDI, in comparison to the other two methods, the ITA method is superior in discovering hidden trends. For instance, according to MK and SR tests, no significant trends are found at all of the stations, however, ITA approach captures a significantly increasing/decreasing trend at stations E26A038 (January and February), E26A012 (January, February, and from May to December) and E26A033 (from June to December)

- According to extreme drought results, the hydrological drought started a few months after the extreme meteorological drought ended. For example, extreme droughts are detected by SPI in the years 1989 (from July to October) and 2000 (November), but not by SPEI during the same period. The SDI also noted the extreme drought in the year 2001 (from March to December). There is a 4-month difference between extreme meteorological drought and hydrological drought. According to correlation analysis, stations 17210 and E26A024 exhibit the highest correlation, whereas 17852 and D26A055 show the lowest correlation.
- The WTC of the monthly SPI/SPEI and SDI indices reveal that, for all in-phase (positively connected), hydrological drought leads to meteorological drought as a result of arrow directions moving to the right-down. Furthermore, the majority of the stations show that positive month signals are highly associated with 12-month time scales. No anti-phase relationships are detected at 12-month time scales.

The results above show that all indices, particularly for longer droughts, can reflect the main droughts in the basin. Accurate long-term data are required for water resource management to solve current and future concerns. With the help of this study, recommendations for sustainable water resource management will be developed to minimize the negative consequences of the basin's drought. Future challenges brought on by socioeconomic and climatic changes may have an impact on the basin's agricultural production and streamflow levels. More research employing innovative techniques is thus needed to resolve this problem.

**Acknowledgements** Acknowledgements are due to state water Works (DSI), general directorate of meteorology (MGM) for providing meteorological data

**Author contributions** M.E. wrote the manuscript, prepared analysis; R.Ç. read and revised manuscript; E.A. prepared good quality figures

**Funding** Not applicable.

**Data availability** The data that support the findings of this study are available from the corresponding author upon request. Due to a

non-disclosure agreement, the data used in the present study are not publicly accessible.

**Code availability** Not applicable.

## Declarations

**Conflict of interest** The authors declare no conflict of interest.

**Ethical approval** Not applicable.

**Consent to participate** Not applicable.

**Consent for publication** Not applicable.

**Informed consent** This study did not include any human participants or animals.

## References

- Abeyasingha NS, Wickramasuriya MG, Meegastenna TJ (2020) Assessment of meteorological and hydrological drought: a case study in Kirindi Oya river basin in Sri Lanka. *Int J Hydrol Sci Technol* 10:429–447. <https://doi.org/10.1504/IJHST.2020.109947>
- Abro MI, Elahi E, Chand R et al (2022) Estimation of a trend of meteorological and hydrological drought over Qinhuai River Basin. *Theor Appl Climatol* 147:1065–1078. <https://doi.org/10.1007/s00704-021-03870-z>
- Achite M, Ceribasi G, Ceyhunlu AI et al (2021) The innovative polygon trend analysis (IPTA) as a simple qualitative method to detect changes in environment—example detecting trends of the total monthly precipitation in semiarid area. *Sustainability* 13:12674. <https://doi.org/10.3390/su132212674>
- Akbari H, Rakhshandehroo GR, Sharifloo AH, Ostadzadeh E (2015) Drought analysis based on standardized precipitation index (SPI) and streamflow drought index (SDI) in Chenar Rahdar river Basin Southern Iran. *Watershed Manag Doi*. <https://doi.org/10.1061/9780784479322.002>
- Akçay F, Kankal M, Şan M (2022) Innovative approaches to the trend assessment of streamflows in the Eastern Black Sea basin, Turkey. *Hydrol Sci J* 67:222–247. <https://doi.org/10.1080/02626667.2021.1998509>
- Alam J, Saha P, Mitra R, Das J (2023) Investigation of spatio-temporal variability of meteorological drought in the Luni River Basin, Rajasthan India. *Arab J Geosci* 16:201. <https://doi.org/10.1007/s12517-023-11290-8>
- Alivi A, Yildiz O, Aktürk G (2021) Investigating the climate change effects on annual average streamflows in the EuphratesTigris basin using the climate elasticity method. *J Fac Eng Archit Gazi Univ* 36:1449–1465
- Bayer Altin T, Altin BN (2021) Response of hydrological drought to meteorological drought in the eastern Mediterranean Basin of Turkey. *J Arid Land* 13:470–486. <https://doi.org/10.1007/s40333-021-0064-7>
- Bhunia P, Das P, Maiti R (2020) Meteorological drought study through spi in three drought prone districts of West Bengal, India. *Earth Syst Environ* 4:43–55. <https://doi.org/10.1007/s41748-019-00137-6>
- Cao S, Zhang L, He Y et al (2022) Effects and contributions of meteorological drought on agricultural drought under different climatic zones and vegetation types in Northwest China. *Sci Total Environ* 821:153270. <https://doi.org/10.1016/j.scitotenv.2022.153270>

- Chang L-L, Niu G-Y (2023) The impacts of interannual climate variability on the declining trend in terrestrial water storage over the Tigris-Euphrates river basin. *J Hydrometeorol* 24:549–560. <https://doi.org/10.1175/JHM-D-22-0026.1>
- Cheraghalizadeh M, Ghameshlou AN, Bazrafshan J, Bazrafshan O (2018) A copula-based joint meteorological–hydrological drought index in a humid region (Kasilian basin, North Iran). *Arab J Geosci* 11:300. <https://doi.org/10.1007/s12517-018-3671-7>
- Christian JI, Basara JB, Hunt ED et al (2021) Global distribution, trends, and drivers of flash drought occurrence. *Nat Commun* 12:6330. <https://doi.org/10.1038/s41467-021-26692-z>
- Danandeh Mehr A, Sorman AU, Kahya E, Hesami Afshar M (2020) Climate change impacts on meteorological drought using SPI and SPEI: case study of Ankara, Turkey. *Hydrol Sci J* 65:254–268. <https://doi.org/10.1080/02626667.2019.1691218>
- Ding Y, Gong X, Xing Z et al (2021) Attribution of meteorological, hydrological and agricultural drought propagation in different climatic regions of China. *Agric Water Manag* 255:106996. <https://doi.org/10.1016/j.agwat.2021.106996>
- Dlamini T, Songsom V, Koedsin W, Ritchie RJ (2022) Intensity, duration and spatial coverage of aridity during meteorological drought years over northeast Thailand. *Climate* 10:137. <https://doi.org/10.3390/cli10100137>
- Edossa DC, Babel MS, Das Gupta A (2010) Drought analysis in the Awash river basin, Ethiopia. *Water Resour Manag* 24:1441–1460. <https://doi.org/10.1007/s11269-009-9508-0>
- Elouissi A, Benzater B, Dabanli I et al (2021) Drought investigation and trend assessment in Macta watershed (Algeria) by SPI and ITA methodology. *Arab J Geosci* 14:1329. <https://doi.org/10.1007/s12517-021-07670-7>
- Farris S, Deidda R, Viola F, Mascaro G (2021) On the role of serial correlation and field significance in detecting changes in extreme precipitation frequency. *Water Resour Res* 57:e2021WR030172. <https://doi.org/10.1029/2021WR030172>
- Farrokhi A, Farzin S, Mousavi S-F (2021) Meteorological drought analysis in response to climate change conditions, based on combined four-dimensional vine copulas and data mining (VC-DM). *J Hydrol* 603:127135. <https://doi.org/10.1016/j.jhydrol.2021.127135>
- Gidey E, Dikinya O, Sebege R et al (2018) Modeling the spatio-temporal meteorological drought characteristics using the standardized precipitation index (SPI) in Raya and its environs, Northern Ethiopia. *Earth Syst Environ* 2:281–292. <https://doi.org/10.1007/s41748-018-0057-7>
- Grinsted A, Moore JC, Jevrejeva S (2004) Application of the cross wavelet transform and wavelet coherence to geophysical time series. *Nonlinear Process Geophys* 11:561–566. <https://doi.org/10.5194/npg-11-561-2004>
- Gumus V, Simsek O, Avsaroglu Y, Agun B (2021) Spatio-temporal trend analysis of drought in the GAP Region, Turkey. *Nat Hazards* 109:1759–1776. <https://doi.org/10.1007/s11069-021-04897-1>
- Gumus V, Avsaroglu Y, Simsek O (2022) Streamflow trends in the Tigris river basin using Mann–Kendall and innovative trend analysis methods. *J Earth Syst Sci* 131:34. <https://doi.org/10.1007/s12040-021-01770-4>
- Han X, Wu J, Zhou H et al (2020) Intensification of historical drought over China based on a multi-model drought index. *Int J Climatol* 40:5407–5419. <https://doi.org/10.1002/joc.6527>
- Hisdal H, Tallaksen LM (2003) Estimation of regional meteorological and hydrological drought characteristics: a case study for Denmark. *J Hydrol* 281:230–247. [https://doi.org/10.1016/S0022-1694\(03\)00233-6](https://doi.org/10.1016/S0022-1694(03)00233-6)
- Jahangir MH, Yarahmadi Y (2020) Hydrological drought analyzing and monitoring by using Streamflow Drought Index (SDI) (case study: Lorestan, Iran). *Arab J Geosci* 13:110. <https://doi.org/10.1007/s12517-020-5059-8>
- Katipoğlu OM (2022) Analysis of spatial variation of temperature trends in the semiarid Euphrates basin using statistical approaches. *Acta Geophys* 70:1899–1921. <https://doi.org/10.1007/s11600-022-00819-2>
- Katipoğlu OM, Acar R (2022) Space-time variations of hydrological drought severities and trends in the semi-arid Euphrates Basin, Turkey. *Stoch Environ Res Risk Assess* 36:4017–4040. <https://doi.org/10.1007/s00477-022-02246-7>
- Kendall MG (1975) Rank correlation methods. Griffin, London
- Khalili D, Farnoud T, Jamshidi H et al (2011) Comparability analyses of the SPI and RDI meteorological drought indices in different climatic zones. *Water Resour Manag* 25:1737–1757. <https://doi.org/10.1007/s11269-010-9772-z>
- King-Okumu C, Tsegai D, Pandey RP, Rees G (2020) Less to lose? Drought impact and vulnerability assessment in disadvantaged regions. *Water* 12:1136. <https://doi.org/10.3390/w12041136>
- Lin Q, Wu Z, Zhang Y et al (2023) Propagation from meteorological to hydrological drought and its application to drought prediction in the Xijiang River basin, South China. *J Hydrol* 617:128889. <https://doi.org/10.1016/j.jhydrol.2022.128889>
- Lorenzo-Lacruz J, Vicente-Serrano SM, González-Hidalgo JC et al (2013) Hydrological drought response to meteorological drought in the Iberian Peninsula. *Climate Res* 58:117–131. <https://doi.org/10.3354/cr01177>
- Ma L, Huang Q, Huang S et al (2021) Propagation dynamics and causes of hydrological drought in response to meteorological drought at seasonal timescales. *Hydrol Res* 53:193–205. <https://doi.org/10.2166/nh.2021.006>
- Malik A, Kumar A, Singh RP (2019) Application of heuristic approaches for prediction of hydrological drought using multi-scalar streamflow drought index. *Water Resour Manag* 33:3985–4006. <https://doi.org/10.1007/s11269-019-02350-4>
- Malik A, Kumar A, Salih SQ, Yaseen ZM (2021) Hydrological drought investigation using streamflow drought index. In: Deo RC, Samui P, Kisi O, Yaseen ZM (eds) *Intelligent data analytics for decision-support systems in hazard mitigation: theory and practice of hazard mitigation*. Springer, Singapore, pp 63–88
- McKee TB, Doesken NJ, Kleist J (1993) The relationship of drought frequency and duration to time scales. *Am Meteorol Soc* 17:179–183
- Meresa H, Zhang Y, Tian J, Abrar Faiz M (2023) Understanding the role of catchment and climate characteristics in the propagation of meteorological to hydrological drought. *J Hydrol* 617:128967. <https://doi.org/10.1016/j.jhydrol.2022.128967>
- Mishra V, Cherkauer KA, Shukla S (2010) Assessment of drought due to historic climate variability and projected future climate change in the midwestern United States. *J Hydrometeorol* 11:46–68. <https://doi.org/10.1175/2009JHM1156.1>
- Mohammed S, Alsafadi K, Enaruvbe GO et al (2022) Assessing the impacts of agricultural drought (SPI/SPEI) on maize and wheat yields across Hungary. *Sci Rep* 12:8838. <https://doi.org/10.1038/s41598-022-12799-w>
- Nalbantis I (2008) Evaluation of a hydrological drought index. *Eur Water* 23(24):67–77
- Nalbantis I, Tsakiris G (2009) Assessment of hydrological drought revisited. *Water Resour Manag* 23:881–897. <https://doi.org/10.1007/s11269-008-9305-1>
- Pang Z, Wang Z (2021) Temperature trend analysis and extreme high temperature prediction based on weighted Markov Model in Lanzhou. *Nat Hazards* 108:891–906. <https://doi.org/10.1007/s11069-021-04711-y>
- Paulo AA, Pereira LS (2006) Drought concepts and characterization. *Water Int* 31:37–49. <https://doi.org/10.1080/02508060608691913>
- Pei J, Deng L, Song S et al (2019) Towards artificial general intelligence with hybrid Tianjic chip architecture. *Nature* 572:106–111. <https://doi.org/10.1038/s41586-019-1424-8>

- Salimi H, Asadi E, Darbandi S (2021) Meteorological and hydrological drought monitoring using several drought indices. *Appl Water Sci* 11:11. <https://doi.org/10.1007/s13201-020-01345-6>
- Şen Z (2012) Innovative trend analysis methodology. *J Hydrol Eng* 17:1042–1046. [https://doi.org/10.1061/\(ASCE\)HE.1943-5584.0000556](https://doi.org/10.1061/(ASCE)HE.1943-5584.0000556)
- Şen Z (2017) Innovative trend significance test and applications. *Theor Appl Climatol* 127:939–947. <https://doi.org/10.1007/s00704-015-1681-x>
- Şen Z, Şişman E, Dabanlı I (2019) Innovative polygon trend analysis (IPTA) and applications. *J Hydrol* 575:202–210. <https://doi.org/10.1016/j.jhydrol.2019.05.028>
- Sharafati A, Nabaei S, Shahid S (2020) Spatial assessment of meteorological drought features over different climate regions in Iran. *Int J Climatol* 40:1864–1884. <https://doi.org/10.1002/joc.6307>
- Sheffield J, Goteti G, Wen F, Wood EF (2004) A simulated soil moisture based drought analysis for the United States. *J Geophys Res.* <https://doi.org/10.1029/2004JD005182>
- Tabari H, Grismer ME, Trajkovic S (2013) Comparative analysis of 31 reference evapotranspiration methods under humid conditions. *Irrig Sci* 31:107–117. <https://doi.org/10.1007/s00271-011-0295-z>
- Tabrizi AA, Khalili D, Kamgar-Haghighi AA, Zand-Parsa S (2010) Utilization of time-based meteorological droughts to investigate occurrence of streamflow droughts. *Water Resour Manage* 24:4287–4306. <https://doi.org/10.1007/s11269-010-9659-z>
- Tang H, Wen T, Shi P et al (2021) Analysis of characteristics of hydrological and meteorological drought evolution in southwest China. *Water* 13:1846. <https://doi.org/10.3390/w13131846>
- Tareke KA, Awoke AG (2022) Hydrological drought analysis using streamflow drought index (SDI) in Ethiopia. *Adv Meteorol* 2022:e7067951. <https://doi.org/10.1155/2022/7067951>
- Tigkas D, Vangelis H, Tsakiris G (2012) Drought and climatic change impact on streamflow in small watersheds. *Sci Total Environ* 440:33–41. <https://doi.org/10.1016/j.scitotenv.2012.08.035>
- Torrence C, Webster PJ (1999) Interdecadal changes in the ENSO–monsoon system. *J Clim* 12:2679–2690. [https://doi.org/10.1175/1520-0442\(1999\)012%3c2679:ICITEM%3e2.0.CO;2](https://doi.org/10.1175/1520-0442(1999)012%3c2679:ICITEM%3e2.0.CO;2)
- Vicente-Serrano SM, Beguería S, López-Moreno JI (2010) A multi-scalar drought index sensitive to global warming: the standardized precipitation evapotranspiration index. *J Clim* 23:1696–1718. <https://doi.org/10.1175/2009JCLI2909.1>
- Wang H, Pan Y, Chen Y (2017) Comparison of three drought indices and their evolutionary characteristics in the arid region of northwestern China. *Atmos Sci Lett* 18:132–139. <https://doi.org/10.1002/asl.735>
- Wang F, Wang Z, Yang H et al (2020) Comprehensive evaluation of hydrological drought and its relationships with meteorological drought in the Yellow River basin, China. *J Hydrol* 584:1751. <https://doi.org/10.1016/j.jhydrol.2020.124751>
- WEF (2020) 5 droughts that changed human history. In: World Economic Forum. <https://www.weforum.org/agenda/2019/05/5-droughts-that-changed-human-history/>. Accessed 23 Feb 2020
- Wilhite D (2000) Chapt drought as a natural hazard: concepts and definitions. Drought Mitigation Center Faculty Publications
- Wilhite DA, Glantz MH (1985) Understanding: the drought phenomenon: the role of definitions. *Water International* 10:111–120. <https://doi.org/10.1080/02508068508686328>
- Wu J, Chen X, Yao H et al (2017) Non-linear relationship of hydrological drought responding to meteorological drought and impact of a large reservoir. *J Hydrol* 551:495–507. <https://doi.org/10.1016/j.jhydrol.2017.06.029>
- Xu Z, Wu Z, He H et al (2019) Evaluating the accuracy of MSWEP V2.1 and its performance for drought monitoring over mainland China. *Atmos Res* 226:17–31. <https://doi.org/10.1016/j.atmosres.2019.04.008>
- Yeh H-F (2019) Using integrated meteorological and hydrological indices to assess drought characteristics in southern Taiwan. *Hydrol Res* 50:901–914. <https://doi.org/10.2166/nh.2019.120>
- Yılmaz M, Alp H, Tosunoğlu F et al (2022) Impact of climate change on meteorological and hydrological droughts for Upper Coruh Basin, Turkey. *Nat Hazards* 112:1039–1063. <https://doi.org/10.1007/s11069-022-05217-x>
- Yuan X, Zhang M, Wang L, Zhou T (2017) Understanding and seasonal forecasting of hydrological drought in the anthropocene. *Hydrol Earth Syst Sci* 21:5477–5492. <https://doi.org/10.5194/hess-21-5477-2017>
- Yuce MI, Esit M (2021) Drought monitoring in Ceyhan Basin, Turkey. *J Appl Water Eng Res* 9:293–314. <https://doi.org/10.1080/23249676.2021.1932616>
- Yuce MI, Deger IH, Esit M (2023) Hydrological drought analysis of Yeşilirmak Basin of Turkey by streamflow drought index (SDI) and innovative trend analysis (ITA). *Theor Appl Climatol.* <https://doi.org/10.1007/s00704-023-04545-7>
- Yue S, Pilon P, Cavadias G (2002a) Power of the Mann-Kendall and Spearman's rho tests for detecting monotonic trends in hydrological series. *J Hydrol* 259:254–271. [https://doi.org/10.1016/S0022-1694\(01\)00594-7](https://doi.org/10.1016/S0022-1694(01)00594-7)
- Yue S, Pilon P, Phinney B, Cavadias G (2002b) The influence of autocorrelation on the ability to detect trend in hydrological series. *Hydrol Process* 16:1807–1829. <https://doi.org/10.1002/hyp.1095>
- Zhang T, Su X, Zhang G et al (2022) Evaluation of the impacts of human activities on propagation from meteorological drought to hydrological drought in the Weihe River Basin China. *Sci Tot Environ* 819:153030. <https://doi.org/10.1016/j.scitotenv.2022.153030>
- Zhou Z, Shi H, Fu Q et al (2020) Assessing spatiotemporal characteristics of drought and its effects on climate-induced yield of maize in Northeast China. *J Hydrol* 588:125097. <https://doi.org/10.1016/j.jhydrol.2020.125097>
- Zhou Z, Shi H, Fu Q et al (2021) Characteristics of propagation from meteorological drought to hydrological drought in the pearl river basin. *J Geophys Res* 126:e2020JD033959. <https://doi.org/10.1029/2020JD033959>

**Publisher's Note** Springer Nature remains neutral with regard to jurisdictional claims in published maps and institutional affiliations.

Springer Nature or its licensor (e.g. a society or other partner) holds exclusive rights to this article under a publishing agreement with the author(s) or other rightsholder(s); author self-archiving of the accepted manuscript version of this article is solely governed by the terms of such publishing agreement and applicable law.